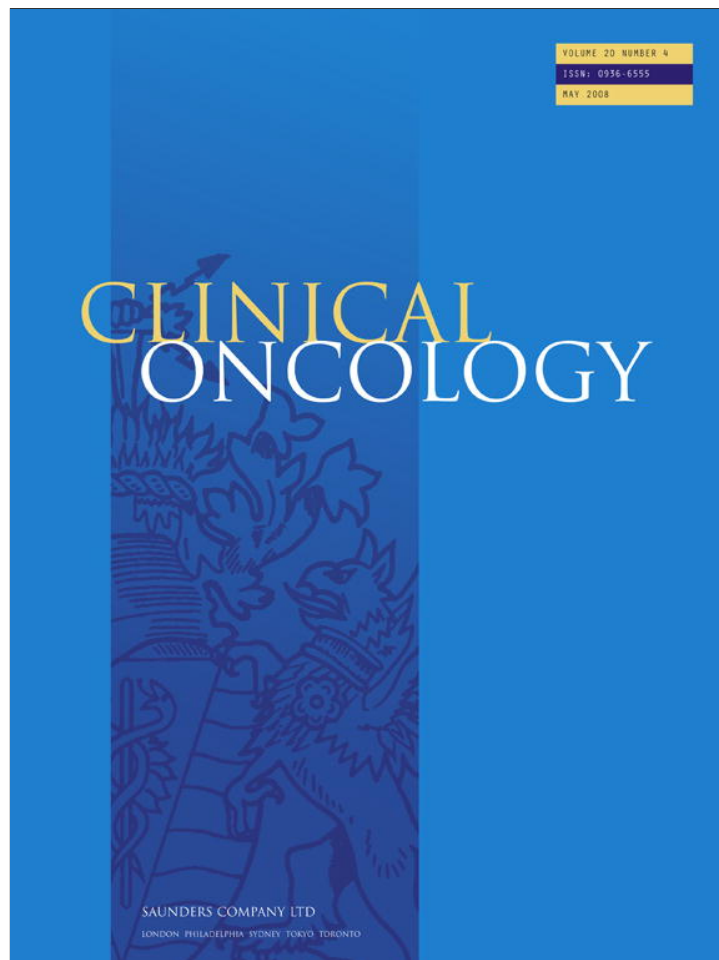


Provided for non-commercial research and education use.
Not for reproduction, distribution or commercial use.



This article appeared in a journal published by Elsevier. The attached copy is furnished to the author for internal non-commercial research and education use, including for instruction at the authors institution and sharing with colleagues.

Other uses, including reproduction and distribution, or selling or licensing copies, or posting to personal, institutional or third party websites are prohibited.

In most cases authors are permitted to post their version of the article (e.g. in Word or Tex form) to their personal website or institutional repository. Authors requiring further information regarding Elsevier's archiving and manuscript policies are encouraged to visit:

<http://www.elsevier.com/copyright>

Original Article

Velocity of Radial Expansion of Contrast-enhancing Gliomas and the Effectiveness of Radiotherapy in Individual Patients: a Proof of Principle

K. R. Swanson*, H. L. P. Harpold*, D. L. Peacock*, R. Rockne*,
C. Pennington†, L. Kilbride†, R. Grant†, J. M. Wardlaw†, E. C. Alvord Jr*

*Laboratory of Neuropathology, University of Washington, Seattle, WA, USA; †Department of Clinical Neurosciences, Western General Hospital, University of Edinburgh, Edinburgh, UK

ABSTRACT:

Aims: The initial aims were to use recently available observations of glioblastomas (as part of a previous study) that had been imaged twice without intervening treatment before receiving radiotherapy in order to obtain quantitative measures of glioma growth and invasion according to a new bio-mathematical model. The results were so interesting as to raise the question whether the degree of radio-sensitivity of each tumour could be estimated by comparing the model-predicted and actual durations of survival and total numbers of glioma cells after radiotherapy.

Materials and methods: The gadolinium-enhanced T1-weighted and T2-weighted magnetic resonance imaging volumes were segmented and used to calculate the velocity of radial expansion (v) and the net rates of proliferation (ρ) and invasion/dispersal (D) for each patient according to the bio-mathematical model.

Results: The ranges of the values of v , D and ρ show that glioblastomas, although clustering at the high end of rates, vary widely one from the other. The effects of X-ray therapy varied from patient to patient. About half survived as predicted without treatment, indicating radio-resistance of these tumours. The other half survived up to about twice as long as predicted without treatment and could have had a corresponding loss of glioma cells, indicating some degree of radio-sensitivity. These results approach the historical estimates that radiotherapy can double survival of the average patient with a glioblastoma.

Conclusions: These cases are among the first for which values of v , D and ρ have been calculated for glioblastomas. The results constitute a 'proof of principle' by combining our bio-mathematical model for glioma growth and invasion with pre-treatment imaging observations to provide a new tool showing that individual glioblastomas may be identified as having been radio-resistant or radio-sensitive. Swanson, K. R. *et al.* (2008). *Clinical Oncology* 20, 301–308

© 2008 The Royal College of Radiologists. Published by Elsevier Ltd. All rights reserved.

Key words: Bio-mathematical model, glioblastoma, invasion, proliferation, radio-sensitivity, radiation therapy

Introduction

Radiation therapy has generally been considered to double the average survival time of patients with glioblastoma based on comparisons of large groups of patients [1], even those subjected to massive resection [2]. This overall or average conclusion contrasts with the observation that some tumours respond to radiation therapy and other do not, which is almost certainly due to there existing a spectrum of radio-sensitivity among such tumours. Hitherto, however, there has not been any way to determine where, along this spectrum, any given tumour lies.

The recent development of a bio-mathematical model of glioma growth [3,4] has provided a theoretical way to create a virtual control for each individual patient for comparison *in vivo* and in real time. The model is neither statistical nor purely theoretical, but is a relatively

straight-forward mathematical translation of the classical biological definition of cancer as uncontrolled proliferation of cells with the capacity to invade locally and metastasise distantly. Because gliomas practically never metastasise, the model can be simplified so that the behaviour of individual gliomas can be defined by two dominant factors, the net rates of proliferation (ρ) and infiltration or diffusion (D). These are the 'final common paths' of innumerable metabolic complexities that occur up-stream and are automatically accounted for in the 'net rates' that cannot be calculated directly but are conceptual end results.

One of the strong points of the model is that the product of these two rates forms the basis of Fisher's well-known approximation [5] for the model-predicted constant velocity of radial expansion of the visible tumour: $v = 2\sqrt{D\rho}$. This has been studied mathematically for many decades as the 'KPP equation' [6–9] and has been found recently to be

applicable to both low- and high-grade gliomas [10–13]. By contrast, the classical exponential model with a constant volume-doubling time fails a priori for gliomas because of the unknown fraction of invisible infiltrating cells, leaving a complementary, but unknown, fraction of visible cells to be observed. An analogy is that of an iceberg with a detectable component above the water and an invisible component below the water. In the new model, although the total number of glioma cells (spread out throughout the brain) may double exponentially, the velocity of the radial growth of the visible mass is linear and constant (not exponential), resulting in an observable mass with an average radius growing approximately linearly in time. This model, combining cellular proliferation and invasion in defining the growth of the visible (bulk) tumour, makes the classical concept of simple exponential growth of the visible mass (with a constant volume-doubling time) unrealistic. The important factor is the constant velocity of radial expansion resulting in a linear plot of the average radius of the imageable tumour vs time despite the spatial complexity involved in human brain tumours.

The velocity of radial expansion can be estimated from two sets of magnetic resonance images (MRIs) without intervening treatment, a common clinical occurrence in the follow-up of low-grade gliomas [10,12], but a rare one in the current management of patients with high-grade gliomas [11]. The recent publication of a study [14] of a group of patients with postoperative and pre-radiation therapy MRIs separated by an interval of 15–53 days without specific oncological treatment provided the present opportunity to measure their growth velocities, to calculate D and ρ explicitly, and to study the possible effects of radiation therapy on individual patients with high-grade gliomas.

Materials and Methods

Mathematical Model

The mathematical model [4] is based on the classical definition of cancer as uncontrolled proliferation of cells with the capacity to invade locally and metastasise distantly. Because gliomas practically never metastasise, the model can be simplified, requiring only the rates of proliferation (ρ) and diffusion (D) to quantify and predict the behaviour of any individual glioma. If we let $c(x,t)$ be the concentration (cells/mm³) of glioma cells at any position x and time t , the following word and mathematical equations can be written:

Rate of change of glioma cell concentration
 = net dispersal of glioma cells
 + net proliferation of glioma cells

$$\partial c / \partial t = \nabla \cdot (D(x) \nabla c) + \rho c (1 - (c/K))$$

D (mm²/year) represents the Fickian random dispersal or net migration rate of glioma cells in undifferentiated brain

tissue: $D(x) = D_g$ is the constant rate of dispersal of glioma cells at a location x in grey matter and $D(x) = D_w$ is another constant rate associated with glioma cells at a location x in white matter. D is mathematically a diffusion coefficient and is a measure of the spread (in units of area per unit time). This migration rate in white matter is generally thought to be faster than that in grey matter: $D_w > D_g$ [15]. A factor of 5 has been used, but we expect that may vary from patient to patient [4]. The parameter ρ (1/year) represents the net rate of proliferation or increase in number of tumour cells, including mitosis and apoptosis. K represents the carrying capacity of the tissue, providing an upper limit on the number of tumour cells capable of occupying any cubic millimetre of brain. The symbol ∇ represents the Laplacian operator, and determines the spatial distribution of tumour cells in the brain. The concentration of cells at the edge of the tumour as visualised on the T1-weighted post-contrast (T1Gd) image has been arbitrarily set at 80% of K and at the edge of the T2-weighted (T2) image at 1.6% [4], approximating the observations of Kelly [16], Kelly *et al.* [17] and Dalrymple *et al.* [18].

The model uses only routine clinical sequences of MRIs and incorporates no other factors (age, performance status, histological type and grade, etc), but can incorporate directionality [19] and concentration [4] of white matter when appropriate. The assumption is that it is the behaviour of the tumour itself that is of interest in an otherwise healthy individual and that any other statistically defined risk factors can only act to decrease the duration of actual survival, completely independent of any calculated virtual duration of survival.

Patient Population

Of the 12 patients recruited [14], 10 had MRIs available electronically. Nine were glioblastomas and one was an anaplastic oligodendroglioma. The images included gadolinium-enhanced T1-weighted (T1Gd) and T2-weighted (T2) images obtained 2–3 days postoperatively and again 2 days before radiation therapy in all patients except one, who did not have a postoperative T1Gd image. The anaplastic oligodendroglioma had an extensive resection that left very little tumour. Thus, there were eight patients who qualified for the present study (numbers 1, 4, 7–12).

The eight patients were relatively homogeneous, having had either a biopsy only (numbers 10 and 12) or a 'debulking' that left most of the T1Gd image intact in the postoperative MRI. Except for relief of increased intracranial pressure, such a 'subtotal resection' was predicted by Woodward *et al.* [20] and found by Lacroix *et al.* [21] to have no significant effect on the duration of survival. Of these eight patients, two (numbers 1 and 7) had no radiation therapy and six received the routine course of radiation therapy, which consisted of 60 Gy in 30 fractions [14]. For the purpose of this study, the effect, if any, of any (salvage) chemotherapy in three patients (numbers 4, 8 and 11) was not considered.

Defining Magnetic Resonance Imaging Abnormality

MRI abnormalities were defined using an in-house, semi-automated tumour segmentation program executed in MATLAB, which combined a thresholding algorithm [22] and a background subtraction algorithm to allow the user to define a region of interest that contains only those pixels that contain tumour. The sum of the series of segmented two-dimensional areas produces a gross tumour volume. This method relies heavily on user judgement of optimal background subtraction and definition of the region of interest, but is also highly reproducible once the threshold value has been chosen. The gross tumour volume was taken as the average of two measurements made by independent observers.

The mean radius was calculated from the gross tumour volume by assuming a sphere of equivalent volume. Inter-observer variation in tumour segmentation with the semi-automated technique has been equal to that of completely manual delineation [23,24] with a typical standard deviation of the radius of 0.5 mm.

Statistical Analysis

The statistical analysis was carried out using SPLUS. The significance of correlations was assessed with a two-tailed correlation test of the hypothesis that the correlation was 0.

Results

As shown in Table 1, the mean T1Gd and T2 radii were derived from spheres of volumes equivalent to the volumes measured on the MRIs. The difference between the T1Gd radii over the time interval between the two sets of MRIs

allowed calculation of the velocity (v) of radial expansion in the interval between operation and radiation treatment, during which time no further treatment was being given, except steroids. This velocity was entered into Fisher's approximation ($v = 2\sqrt{D\rho}$). The T1Gd and T2 radii for each date provided the basis for the calculation of D/ρ , an 'index of invisibility' [4]. The two equations in the two unknowns, D and ρ – one involving the product and the other the ratio – allowed calculation of their respective values. Although v can be calculated only once (at the end of the time interval), D/ρ can be calculated at each time point, using a pair of T1Gd and T2 MRI observations and can be used with v to calculate D and ρ for each date. Ideally, of course, these pairs of values at each end of the time interval should be identical. Actually, however, some were quite different; most frequently the value of D/ρ decreased, suggesting that steroids may have decreased some oedema included in the T2 volume, but generally the average was accepted.

Segmentation errors in the MRI-defined volumes propagate as errors first to the calculated radii and then to the velocity, the ratio D/ρ , and the final calculation of D and ρ . Data shown in the tables and figures include a ± 1 standard deviation error in the MRI-defined radii of 0.5 mm. On average, this generates a 69–101% variation in D/ρ , $\pm 55\%$ in D and $\pm 35\%$ in ρ . These uncertainties propagate, in turn, to the other calculated items in the tables and figures.

A univariate statistical analysis of this small population considered (Pearson) correlations of the covariates with actual survival from the time of the final MRI 2–3 days after operation (Table 2). No significant correlation with survival was found for age in this population, but significant correlations with actual survival were found for mean T1Gd radius, T1Gd velocity, average ρ , and burden (of glioma cells) at diagnosis.

Table 1 – Radii of spheres equivalent to the volumes measured on T1Gd and T2 magnetic resonance images enabled the calculation of velocity, ρ and D (all values rounded to the nearest 0.1)

Patient	Day	Radii (mm)		T1Gd velocity (mm/year)	D/ρ (mm ²)	D (mm ² /year)	ρ (1/year)
		T1Gd (± 0.5 mm)	T2 (± 0.5 mm)				
1	0	23.6	33.1	113.1 (93.3–133.8)	2.4	88.0	36.5
	18	29.2	35.6				
4	0	10.3	14.5	25.9 (15.5–37.6)	0.4	8.5	19.8
	33	12.7	18.6				
7	0	20.2	26.0	90.8 (65.7–114.4)	0.9	42.2	48.8
	15	23.9	29.9				
8	0	15.3	19.9	26.6 (14.6–38.9)	0.5	9.7	18.3
	30	17.5	22.9				
9	0	16.4	24.1	43.2 (29.5–57.6)	1.6	27.0	17.3
	26	19.5	24.3				
10	0	21.5	26.1	24.0 (12.2–34.3)	0.6	9.1	15.8
	33	23.6	25.9				
11	0	18.1	29.7	23.2 (13.7–31.9)	3.5	21.9	6.3
	40	20.6	23.2				
12	0	20.9	29.9	54.1 (42.9–64.4)	2.2	40.0	18.3
	34	25.9	31.6				

Table 2 – Pearson correlations with actual survival time

Covariate	P value
Age	0.103
T1Gd radius at presentation	0.002
T1Gd velocity	0.006
T2 radius at presentation	0.032
T2 velocity	0.567
Mean D/ρ	0.578
Mean ρ	0.022
Mean D	0.094
Burden at diagnosis	0.014

To predict the duration of survival given the velocity of radial expansion, one needs some measure of the 'fatal tumour burden' (FTB), which we assumed to exist. We considered two hypothetical FTBs – one related to a fatal tumour size on T1Gd MRI and one associated with a fatal number of total glioma cells at death. Both were predicted by simulations of the mathematical model forward in time from the point of diagnosis assuming no significant treatment effects. The resultant 'baseline' model-predicted survival times if untreated were compared with actual survival times of the treated patients. Any increase in actual survival time relative to the model-predicted untreated survival time was hypothesised to represent a possible measure of treatment effect.

Fatal Tumour Burden Defined by Magnetic Resonance Imaging-defined Radius

Our first approximation considered the sizes reached after the survival times of the two patients who received no radiation therapy. Knowing their durations of survival, their velocities of radial expansion and their actual sizes when last measured, we projected (predicted) the radii of their tumours at death to be 32 and 37 mm, an average of about 35 mm, not much different from the 30 mm assumed by Woodward *et al.* [20] and well within the range reported in

autopsies [25,26]. We then assumed that each of the other (treated) patients should have reached this average predicted fatal size, beginning with the actual size when last measured and increasing according to the velocity of radial expansion (measured for each patient), if they had been untreated or if their radiation therapy had been ineffective. We called this duration the 'virtual untreated' duration and calculated the ratio of the two survival times, treated actual to 'virtual untreated', for each patient (Table 3). This ratio could be regarded as an index of radiotherapy effectiveness, 100% representing no effect, or index of radio-sensitivity of that particular tumour, 100% being completely radio-resistant as though radiation therapy had not been given and the patient survived exactly as predicted.

Figure 1a shows the actual patient survival times vs the model-predicted durations of survival (if untreated) for the FTB defined by T1Gd radius (35 mm). The two 'untreated controls' survived 79 and 121% of their average expected survival (Table 3), and only three of the others survived longer: 153, 175 and 276%. The other three X-irradiated patients clearly showed no prolongation of survival, with only 42–126% of the expected survival if untreated, suggesting that these tumours were completely radio-resistant. The effect of chemotherapy, ignored for the purpose of this study, must have been rather slight, only one of three patients showing as much as 153% of the expected survival if untreated.

Fatal Tumour Burden Defined by Total Number of Glioma Cells

Because the above calculations were based only on the velocity and the time to reach an average size on T1Gd MRI, we considered an alternative calculation based on the total number of glioma cells that the individual combination of D and ρ could have produced in the actual survival time available for each patient. Combining each patient's values of D and ρ with the size of the MRI-defined abnormality allowed estimation of the burden of disease (total number of glioma cells within the brain) at the time of diagnosis or

Table 3 – Treatments and survival times (actual 'treated' durations with estimated 'virtual untreated' durations), assuming a fatal tumour burden defined by T1Gd radius of 35 mm

Patient/age/gender	Treatment			Survival time (days)		
	Radiation therapy	Chemotherapy	Other	Estimated (range)	Actual	Actual (%) (range)
1/57/female	0	0	STR debulk	34 (29–42)	27	79 (65–93)
7/58/female	0	0	STR debulk	56 (44–77)	68	121 (88–153)
10/64/male	+	0	Biopsy	194 (133–360)	82	42 (23–62)
12/50/male	+	0	Biopsy	90 (75–112)	157	175 (140–209)
9/22/male	+	0	STR debulk	150 (113–222)	415	276 (187–366)
4/49/female	+	+	STR debulk	336 (236–587)	425	126 (72–180)
8/50/male	+	+	STR debulk	259 (178–476)	397	153 (83–223)
11/71/male	+	+	STR debulk	253 (182–418)	261	103 (63–144)

STR, subtotal resection.

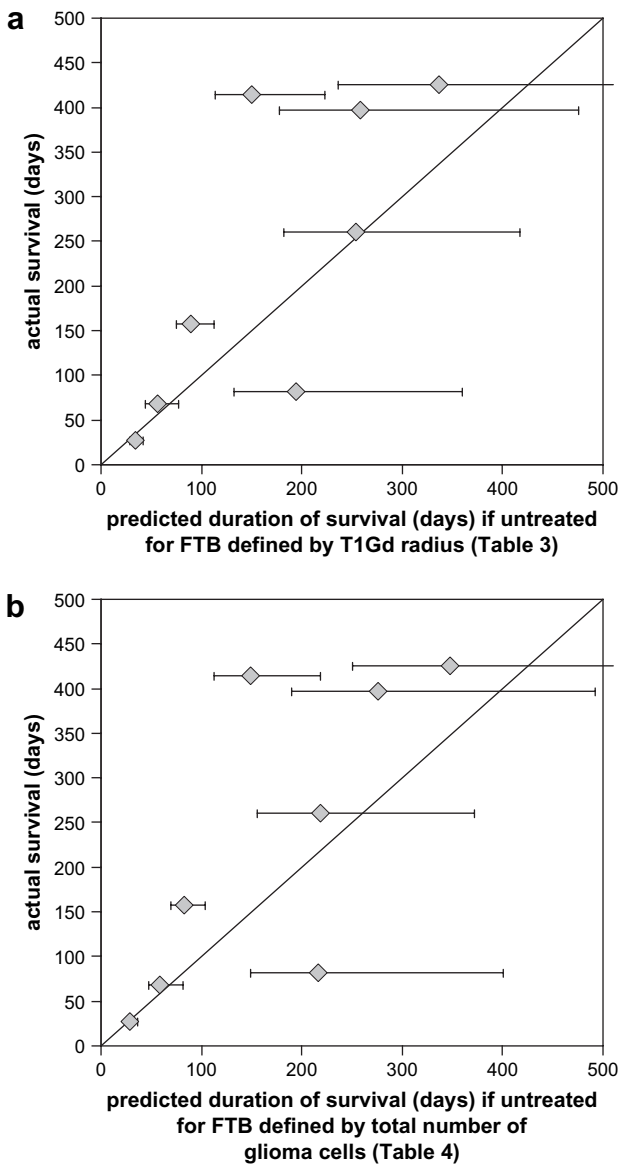


Fig. 1 – (a) Correlation of actual survival time and predicted survival time if untreated for fatal tumour burden defined by T1Gd size (Table 3). (b) Correlation of actual survival time and predicted survival time if untreated for fatal tumour burden defined by total number of glioma cells (Table 4). The two patients in the lower-left were not given XRT.

at any future time. This estimated number of cells was calculated by integrating the solution (c) to the mathematical model (see Materials and Methods) for the given values of the patient-specific model parameters at the size and time of diagnosis and then projecting the number of cells forward in time to the actual time of death. As shown in Table 4, the two ‘untreated controls’ (patient numbers 1 and 7) would have had 1.0 and 1.3×10^{10} cells for an average of about 1.1×10^{10} cells at the actual times of death. The other patients would have had 0.5 – 6.6×10^{10} cells if they had not been treated. Figure 1b shows the actual patient survival times vs the model-predicted

durations of survival (if untreated) for the FTB defined by the total number of glioma cells (1.1×10^{10} cells). Figure 2 shows the model-predicted glioma cell burden (total number of gliomas cells) at death if the patient had been untreated plotted against the increase in actual survival over the model-predicted survival. Assuming that they would have died at the average 1.1×10^{10} cells (dashed line in Fig. 2), we then assumed that the radiation therapy had destroyed enough cells to allow the patient to live longer, shown in Fig. 2 as the percentage increase in actual survival at death over that predicted. As shown in Table 4, the two ‘untreated controls’ (patient numbers 1 and 7) had 93–115% of the expected FTB of total glioma cells, the three best cases 189–279% and the three worst cases 38–142%. Thus, in Fig. 2, the difference between the solid trend line and the dashed predicted FTB of glioma cells quantifies net cell loss due to the radiotherapy. This cell loss translates into the actual increase in survival over that predicted for each patient.

As shown in Fig. 3, there is a remarkably linear relationship between the two methods of calculating the survival based on each theoretical FTB. Of course, because the velocity is related to the product $D\rho$, the correlation could be predicted, but at least the initial goal of calculating D and ρ can be said to have some inherent value.

Discussion

Several novel features are incorporated in this report. The first and most unusual feature of this series of patients is the availability of the second MRI without intervening treatment [14], allowing the measurement of the velocity of radial expansion of each individual tumour as seen on T1Gd images. This velocity, which is constant with time according to Fisher’s approximation, forms a critical element in the calculation of D and ρ in the new bi-mathematical model [3,4]. Additional features of the T1Gd and T2 images allow the calculation of D/ρ (an index of invisibility) and then the net proliferation rate (ρ) and the net diffusion rate (D). From these rates and sizes we could create a virtual control, untreated, with the same tumour characteristics (size, velocity and index of invisibility), for comparison with the actual patient, treated by radiation therapy and/or various extents of resection [20].

A second unusual and significant feature of this report should be noted: the estimation of a FTB derived from the two ‘untreated’ patients. Two different FTBs could be estimated from these patients: the first based on the size reached by the patient’s measured velocity, and the second based on reaching a fatal total number of glioma cells using the newly calculated values of D and ρ for each patient. These two estimates seemed to be at least relatively independent of each other, the velocity being directly measured from the two sets of MRIs each patient had before radiation therapy, and the values of D and ρ calculated from the combination of the velocity and other characteristics of the individual MRIs. The assumption underlying the first FTB was that each of the other (treated)

Table 4 – Actual ('treated') durations of survival with estimated ('virtual untreated') survival, assuming a fatal tumour burden defined by total number of glioma cells of 1.1×10^{10}

Patient/age/gender	Total number of cells		Survival time (days)		
	at diagnosis ($\times 10^9$)	at death if untreated ($\times 10^{10}$)	estimated (range)	actual	actual (%) (range)
1/57/female	5.1 (4.7–5.3)	1.0 (0.9–1.2)	29 (25–36)	27	93 (75–108)
7/58/female	2.7 (2.5–2.8)	1.3 (0.9–1.7)	59 (47–82)	68	115 (83–145)
10/64/male	2.9 (2.7–3.1)	0.5 (0.4–0.6)	216 (149–401)	82	38 (20–55)
12/50/male	3.7 (3.4–3.9)	2.2 (1.7–2.9)	83 (70–104)	157	189 (151–224)
9/22/male	1.9 (1.7–2.1)	6.6 (3.1–12.0)	149 (113–219)	415	279 (189–367)
4/49/female	0.4 (0.4–0.5)	1.7 (0.6–3.6)	348 (250–588)	425	122 (72–170)
8/50/male	1.2 (1.1–1.3)	2.1 (0.8–4.3)	276 (190–492)	397	144 (81–209)
11/71/male	3.3 (3.1–3.4)	1.3 (0.8–2.0)	218 (156–372)	261	120 (70–167)

patients should have reached this average, untreated, fatal size, beginning with the actual size when first measured and increasing according to the individual's measured actual velocity of radial expansion. That is, each patient should have reached this size if untreated or if the radiation therapy had been ineffective. By contrast, if radiation therapy had been effective, a longer survival should have been noted. The assumption underlying the second FTB was that the radiation therapy might have reduced the total number of glioma cells, the remaining viable cells able to proliferate and invade, producing the same total number of cells, i.e. the average of the two 'untreated controls'. That is, the treated patient could not have survived to produce more tumour cells unless radiation therapy had killed the hypothetical excess. Both calculations yielded percentages above 100% indicating relative effectiveness of radiation

therapy or below 100% indicating resistance of the glioma to radiation therapy. Just how much variation there is in either of the FTBs is not known, but we are collecting cases with all of these factors in mind. To our knowledge, all that has been published is the report of 30 autopsied cases by Concannon *et al.* [25] showing a range in radii of the visible tumour of 15–44 mm with a median of 27 mm, which Woodward *et al.* [20] rounded to 30 mm. Burger *et al.* [26] reported that in three of their 15 autopsy cases, the glioma cells infiltrated more than 30 mm beyond the enhanced-computed tomography border, the dimensions of which were not recorded.

We have developed an independent index of radio-sensitivity, but it requires a third MRI at some time after the radiation therapy [27,28], and such MRIs were not available for the present study. Although age and performance status are well-known statistical predictors of survival [29], they

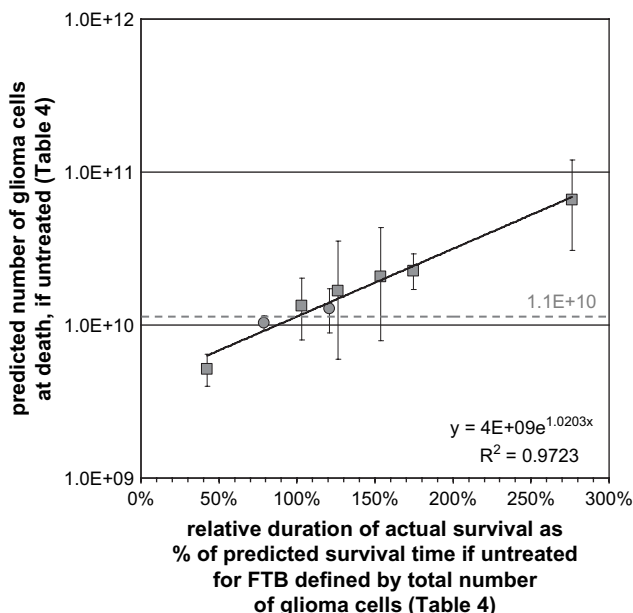


Fig. 2 – Correlation of total number of glioma cells (y axis) predicted at death if untreated (Table 4) with the relative duration of actual survival (x axis) for fatal tumour burden defined by T1Gd size (Table 3).

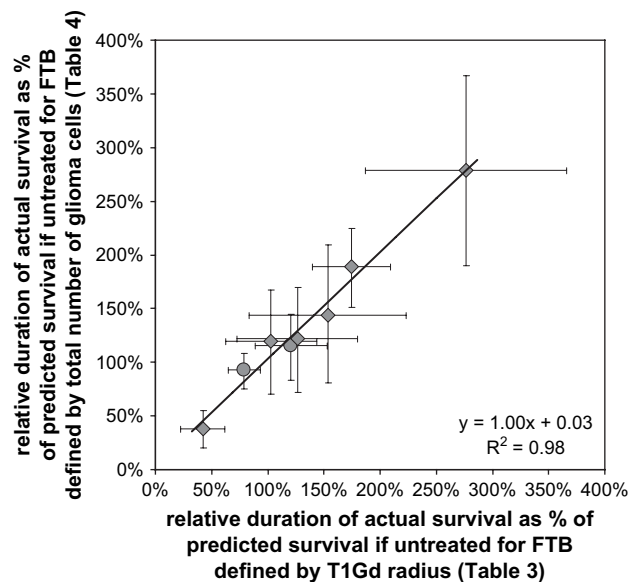


Fig. 3 – Correlation of relative effectiveness of radiation therapy (as a percentage of actual predicted survival if untreated) by two methods of estimating the fatal tumour burden: (1) x axis: by a fatal size (35 mm radius on T1Gd: Table 3) and (2) y axis: by a fatal total number of glioma cells (1.1×10^{10} cells: Table 4).

do not enter into the mathematical model, which is based solely on the two critical factors (D and ρ) defining the behaviour of the individual tumour. In other words, the model assumes that the patient is generally healthy; any adverse risk factors can only decrease the actual survival duration. Such would be important if toxicity of the putative treatment were being investigated, but is irrelevant if any benefit is being sought.

One of the shortcomings of the present report is the shortness of the interval between the two MRIs, potentially leading to only small differences in the volumes measured (and the radii calculated) and, therefore, to inaccuracies in the calculations of the velocity. With inherent errors in the measuring techniques leading to typical errors of ± 0.5 mm in the radius, radial differences of only 1 or 2 mm are pushing up against the limits, and these differences in two MRIs separated by 30 days without treatment represent radial velocities of 12–24 mm/year, at the lower boundary that we have found for high-grade gliomas [13]. Any shorter interval would have eliminated or, at least, raised serious questions about the accuracy of v as measured in half of the patients in the present series. Other potential sources of error may have had an effect on our estimate of the FTB in the two un-irradiated patients. Some of the patients may have died too soon because the tumour was unusually large at the time of diagnosis with associated oedema and herniation, and both of these may have been aggravated by the acute effects of radiation therapy. Indeed, four of the patients had tumours measuring at least 20 mm in radii, only one having a small tumour (10 mm) and three what we [13,20] have accepted as an average size tumour (15–18 mm). Other diseases (e.g. pulmonary embolism) or a poor combination of older age and poor neurological performance (no data available for the latter) may have contributed to early death. In our bio-mathematical model we have assumed that these statistically adverse factors are not present, that the patients are generally healthy and that only an unfavourable ratio of D/ρ with a predominance of invisibly infiltrating glioma cells would contribute to an early death. In other words, these might not have been the best patients to prove that radiation therapy is not effective, but another specifically designed study could at least use the new tool provided.

Another shortcoming is the postoperative timing of the MRIs with distortion of the tumour geometry such that one may doubt its similarity to spheres. This was certainly the problem with the case of the anaplastic oligodendroglioma subjected to an almost complete resection. The possibility also exists that postoperative changes may obscure the actual mass of growing tumour and render the calculation of v inaccurate. Unfortunately, the ideal of obtaining two MRIs without intervening treatment in the preoperative period is rarely achieved in high-grade gliomas. Another problem is the use of steroids during the 'untreated' course between the two MRIs; indeed, two patients (numbers 10 and 11) showed a decrease in the T2 volume, as though oedema may have been reduced, forcing us to ignore the second T2 in our simulation of the behaviour of these patients' gliomas. One other (number 9) had only a slight

increase in T2 radius, but how much the steroids were responsible remains unknown, although there did not seem to be any other major distortion from the expected courses.

Finally, we want to stress the fact that the present report presents a radically different approach to analysing results. Classical statistical analysis can only say that XRT is beneficial in that the mean survival of patients (in this study) receiving XRT is 5-fold longer than the untreated patients ($p < 0.009$), but cannot say which patients are benefited or by how much. The present approach pushes statistical analyses to the side and emphasises the comparison of individual patients with widely different but measured sizes, rates of proliferation (ρ) and diffusion/dispersal (D) and total numbers of glioma cells (both visible and invisible) with their matched virtual untreated controls. This approach is quite different from the current double-blind randomised clinical trial in which large numbers of patients are assumed to compensate for reliance on only the histopathological diagnosis and the lack of measurement of the different rates of D and ρ , each of which can vary at least 10-fold for high-grade gliomas [13]. That as few as eight patients can show the potential of this mathematical approach in an analysis of the effectiveness of radiation therapy not only represents a 'proof of principle', but also suggests a way to improve the analysis of the effectiveness of other types of treatment that are increasingly being individualised to accommodate advances in molecular-genetic characteristics of individual gliomas.

Opportunities to compare the application of this mathematical model should be sought in large randomised clinical trials – with more patients given a second MRI before the first treatment and more MRIs at appropriate intervals before and after each subsequent treatment. As noted above, radial velocities of 12–24 mm/year are at the lower boundary that we have found for high-grade gliomas and can result from an increase in radii of only 1–2 mm in a month. Current techniques of measurement in routine clinical MRIs can hardly be expected to do better, so that any interval without treatment shorter than 1 month can be expected to miss the most slowly growing high-grade gliomas, the very ones that will probably survive the longest and appear as false positives, appearing to respond to the treatment being tested using current response assessment criteria [30,31]. Better discrimination of radio- or chemo-sensitivities in individual patients *in vivo* and in real time might allow better identification of histological or imaging features or other emerging biomarkers without diluting their effects in the average or median result of a large group of 'similar' patients, whose 'similarity' cannot otherwise be proven.

Conclusion

That some gliomas are relatively radio-sensitive and some relatively radio-resistant has been confirmed in this study of individual patients. The present technique of comparing actual treated patients with their individually matched

untreated virtual controls may permit identifying not only which particular glioma is radio-sensitive and which is radio-resistant, but also the degrees of radio-sensitivity measured on a continuous scale. Whether one wishes to average the numbers of patients responding or to average the degrees to which they responded in order to find a statistically significant conclusion, or whether one wishes to examine each case to discover why each particular tumour responded or not must remain for more specifically designed future studies. At least a new tool is available.

Author for correspondence: K. R. Swanson, Department of Pathology, University of Washington, Harborview Medical Center, 325-9th Avenue (HMC Box 359791), Seattle, WA 98104, USA. Tel: +206-221-6577; E-mail: swanson@amath.washington.edu

Received 14 February 2007; received in revised form 2 January 2008; accepted 3 January 2008

References

- Bloor RJ, Templeton AW, Quick RS. Radiation therapy in the treatment of intracranial tumors. *Am J Roentgenol Radium Ther Nucl Med* 1962;87:463–472.
- Jelsma R, Bucy PC. The treatment of glioblastoma multiforme of the brain. *J Neurosurg* 1967;27:388–400.
- Tracqui P, Cruywagen GC, Woodward DE, et al. A mathematical model of glioma growth: the effect of chemotherapy on spatio-temporal growth. *Cell Prolif* 1995;28:17–31.
- Swanson KR. Mathematical modeling of the growth and control of tumors. Thesis, University of Washington, 1999.
- Fisher RA. The wave of advance of advantageous genes. *Ann Eugenics* 1937;7:353–369.
- Shigesada N, Kawasaki K. *Biological invasions: theory and practice*. Oxford: Oxford University Press; 1997.
- Murray JD. *Mathematical biology I. An introduction*, 3rd edn. New York: Springer; 2002.
- Murray JD. *Mathematical biology II. Spatial models and biological applications*, 3rd ed. New York: Springer; 2003.
- Kolmogoroff A, Petrovsky I, Piscounoff N. Étude de l'équation de la diffusion avec croissance de la quantité de matière et son application à un problème biologique. *Moscow Univ Bull Math* 1937;1:1–25.
- Mandonnet E, Delattre JY, Tanguy ML, et al. Continuous growth of mean tumor diameter in a subset of grade II gliomas. *Ann Neurol* 2003;53:524–528.
- Swanson KR, Rostomily RC, Alvord EC Jr. Confirmation of a theoretical model describing the relative contributions of net growth and dispersal in individual infiltrating gliomas. *Can J Neurol Sci* 2003;30:407.
- Pallud J, Mandonnet E, Duffau H, et al. Prognostic value of initial magnetic resonance imaging growth rates for World Health Organization grade II gliomas. *Ann Neurol* 2006;60:380–383.
- Harpold HLP, Alvord EC Jr, Swanson KR. The evolution of mathematical modeling of glioma growth and invasion. *J Neuropath Exp Neurol* 2007;66:1–9.
- Pennington C, Kilbride L, Grant R, Wardlaw JM. A pilot study of brain tumour growth between radiotherapy planning and delivery. *Clin Oncol* 2006;18:104–108.
- Giese A, Westphal M. Glioma invasion in the central nervous system. *Neurosurgery* 1996;39:235–250 [discussion: 250–252].
- Kelly PJ. Computed tomography and histological limits in glial neoplasms: tumor types and selection for volumetric resection. *Surg Neurol* 1993;39:458–465.
- Kelly PJ, Dumas-Duport C, Kispert DB, et al. Imaging-based stereotaxic serial biopsies in untreated intracranial glial neoplasms. *J Neurosurg* 1987;66:865–874.
- Dalrymple SJ, Parisi JE, Roche PC, et al. Changes in proliferating cell nuclear antigen expression in glioblastoma multiforme cells along stereotactic biopsy trajectory. *J Neurosurg* 1994;35:1036–1044.
- Jbabdi S, Mandonnet E, Duffau H, et al. Diffusion tensor imaging allows anisotropic growth simulations of low-grade gliomas. *Magn Res Med* 2005;54:616–624.
- Woodward DE, Cook J, Tracqui P, et al. A mathematical model of glioma growth: the effect of extent of surgical resection. *Cell Prolif* 1996;29:269–288.
- Lacroix M, Abi-Said D, Fourney DR, et al. A multivariate analysis of 416 patients with glioblastoma multiforme: prognosis, extent of resection, and survival. *J Neurosurg* 2001;95:190–198.
- Ridler TW, Calvard S. Picture thresholding using an iterative selection method. *IEEE Trans Sys Man Cybernet* 1978;8:630–632.
- Vos MJ, Uitdehaag BMJ, Barkhof F, et al. Interobserver variability in the radiological assessment of response to chemotherapy in glioma. *Neurology* 2003;60:826–830.
- Weltens C, Menten J, Feron M, et al. Interobserver variations in gross tumor volume delineation of brain tumors on computed tomography and impact of magnetic resonance imaging. *Radiother Oncol* 2001;60:49–59.
- Concannon JP, Kramer S, Berry R. The extent of intracranial gliomata at autopsy and its relationship to techniques used in radiation therapy of brain tumors. *Am J Roentgenol Radium Ther Nucl Med* 1960;84:99–107.
- Burger PC, Heinz ER, Shibata T, et al. Topographic anatomy and CT correlations in the untreated glioblastoma multiforme. *J Neurosurg* 1988;68:698–704.
- Rockne R, Alvord EC Jr, Rockhill JK, Swanson KR. Modeling radiotherapy effect in glioma patients. *J Math Biol*, in press.
- Swanson KR, Rockne R, Rockhill JK, Alvord EC Jr. Mathematical modeling of radiotherapy in individual glioma patients: quantifying and predicting response to radiation therapy. *AACR Annual Meeting* 2007.
- Scott CB, Scarantino C, Urtasun R, et al. Validation and predictive power of Radiation Therapy Oncology Group (RTOG) recursive partitioning analysis classes for malignant glioma patients: a report using RTOG 90-06. *Int J Radiat Oncol Biol Phys* 1998;40:51–55.
- Galanis E, Buckner JC, Maurer MJ, et al. Validation of neuro-radiologic response assessment in gliomas: measurement by RECIST, two-dimensional, computer-assisted tumor area, and computer-assisted tumor volume methods. *Neuro-oncology* 2005;8:156–165.
- MacDonald DR, Cascino TL, Schold SC Jr, Cirincross JG. Response criteria for phase II studies of supratentorial malignant glioma. *J Clin Oncol* 1990;8:1277–1280.